NGL-05-002-105
NSG-7129

ATMOSPHERIC BLOW-OFF DURING ACCRETION OF THE TERRESTRIAL PLANETARY ATMOSPHERES

AIAA

M.A. Lange and Thomas J. Ahrens

N88-27088
440

Submitted to: ICARUS

Seismological Laboratory
California Institute of Technology
Pasadena, CA 91125

December, 1987

RECEIVED
LIBRARY
1988 MAR -7 P 3:08
AIAA/TIS

(NASA-CR-186429) ATMOSPHERIC BLOW-OFF DURING ACCRETION OF THE TERRESTRIAL PLANETARY ATMOSPHERES (California Inst. of Tech.) 44 p

N90-70904

Unclas
00/91 0270881

ABSTRACT

We present the first model calculations of impact-induced blow-off of an impact-generated atmosphere during accretion of the terestrial planets. Volatile bearing minerals contained in the accreting planetesimals will be degassed upon impact on the growing planet, provided shock pressures in the planetesimal exceed the critical shock pressures required for devolatization. The released gases will give rise to a growing proto-atmosphere on the accreting planet. Also contributing to proto-atmosphere loss are solid-gas reactions with surface material (e.g. re-hydration with anhydrous minerals; reactions between water vapor and metallic iron). However while gas is reacting with hot, possibly molten surface material, the evolving atmosphere is being subject to continuous impacts of infalling planetesimals. This study is focussed on this process. The interaction of bolides with the exponential atmosphere is treated according to a formalism developed for blast waves (Bach et al, 1975; Ahrens and O'Keefe, 1987). We calculate the mass of atmospheric gas accelerated to velocities in excess of the escape velocity of the body and consequently lost to space. Accretion rates, specified according to a Safronov-accretion model yield the number of planetesimals for a given planetesimal size and thus the accumulative effect of the atmospheric blow-off. The major parameters determining whether or not the evolving atmosphere can be retained on the planet are (i) the scale height of the atmosphere (ii) The atmospheric density at the surface of the planet and (iii) the accretion rate as a function of planetary and planetesimal radius.

We find atmospheric impact, as a process, affects the final mass of a primary atmo-

sphere. Moreover for a given atmosphere structure, planetesimals and water content an optimum impactor (planetesimal) size exists, for which impact-induced blow-off efficiency becomes greatest. This optimum radius r^*_{pl}, is approximately 100, 130, and 160 km for Earth, Venus and Mars, respectively. The calculations are based on the assumption that planetesimals contain 1.0% H_2O (by mass) and these planets atmospheric surface temperature is fixed at 800^o K by the solidus of an H_2O-rich magma. For these conditions, while the final amount of atmospheric inventory exceeds the total amount of atmospheric loss due to cratering for the Earth and Venus, on Mars the impact-induced blow-off rates exceed the present atmospheric inventory. This is reflected in the ratio, M^*_{cl}, between final mass of a water atmosphere and total mass of dissipated gases for models with planetesimal radii equal to r^*_{pl}. M^*_{cl} is equal to 1.4, 1.3 and 0.75 for Venus, Earth and Mars respectively. Changing model parameters will not lead to $M^*_{cl} < 1$ for Earth and Venus. Thus, despite atmospheric cratering, an impact-induced primary atmosphere remains a realistic option for Venus and Earth but is less likely for Mars.

1. INTRODUCTION

Previously we have demonstrated that volatile bearing minerals in planetesimals will lose volatiles (H_2O, CO_2) upon impact on a growing planet (Lange and Ahrens, 1982a; 1982b). We have also shown that the loss of atmospheric H_2O and CO_2 by water reaction with anhydrous surface minerals as suggested by Jakosky and Ahrens, (1979) will be overwhelmed by impact-induced degassing towards the end of the accretion period (Lange and Ahrens, 1982a). Moreover, Abe and Matsui (1984, 1986) have demonstrated that the release of large quantities of water during the impact-degassing phase of terrestrial planet accretion leads to sufficiently high temperature, via thermal blanketing, such that magma oceans are initially present on the surfaces of the terrestrial planets. Ringwood (1979) has hypothesized that reactions between water and metallic iron will dominate the atmospheric water budget and will essentially remove all available water, thus accounting for the entire FeO-budget of the Earth. Lange and Ahrens (1984) have demonstrated that a slightly inhomogeneous accretion model with most of the iron accretion taking place in the first $\sim 4/5$ of the accretional period will suffice to allow accumulation of the terrestrial water budget during the later parts of accretion.

Both approaches of the earlier work lead to the formation of a proto-atmosphere/hydrosphere during the later steps of accretion. Such a (predominantly) steam atmosphere however, will be subject to numerous impacts by the still infalling planetesimals as for example recently pointed out by Cameron, (1983). The interaction of the accreting bolides with an evolving, exponential steam atmosphere is the subject of this paper. As discussed in Ahrens et al, (1987) most of this interaction occurs after the bolide

hits the solid planet. The major transfer of energy to the atmosphere is via the impact ejecta as is summarized below. Due to the large difference in the mechanical impedances of water vapor and silicate planetesimals, the continuum treatment of the interaction of relevant processes is difficult. Ahrens and O'Keefe (1987) give a review of appropriate procedures and earlier studies on this subject. One of their major conclusions is that energy transfer to the atmosphere can amount to some 30-40% of the bolide-energy. Even though only $\sim$ 8% of the impactor energy of high energy impactors ($E > 10^{21} J$) is directly partitioned into internal and kinetic energy of the atmosphere, a large fraction of the kinetic energy of the ejecta as well as substantial fractions of target and projectile internal energy is indirectly transferred to atmospheric gases by air drag, radiation and conduction processes, respectively (Ahrens and O'Keefe, 1987). Thus, most of the energy exchange takes place relatively close to the target surface. However, the exact nature of the interaction depends on bolide energy and smaller, low energy impactors will lose most of their energy on their way through the atmosphere. Ahrens and O'Keefe [1987] conclude from these findings that large energy impacts into an atmosphere can be approximated by a formalism developed for blast waves in exponential atmospheres (Zel'dovich and Raizer, 1967). Bach et al., [1975] also investigated this problem and developed solutions for a number of non-dimensional similarity variables relevant to this problem. These solutions are used by Ahrens and O'Keefe [1987] to obtain quantitative estimates on blow-off efficiencies (i.e., the mass fraction of total atmospheric mass accelerated to velocities in excess of the planetary escape velocity) for a terrestrial atmosphere but for varying escape velocities.

In this study, we will also utilize the Bach et al., [1975] findings in considering the possible dissipation of an early proto atmosphere by infalling planetesimals in the late stages of accretion of the terrestrial planets (Venus, Earth and Mars). However, instead of using atmospheric parameters relevant for the present terrestrial atmosphere, we will derive these parameters for an evolving water vapor atmosphere. Since the efficiency of atmospheric dissipation depends critically on atmosphere properties, complex feedbacks between the formation of a proto-atmosphere and its subsequent possible loss by planetesimal impact are expected. In addition, the Ahrens and O'Keefe [1987] results imply that this process might also be controlled by the size distribution of accreting bolides. They found that for a given atmospheric structure there is an impactor energy for which blow-off efficiencies approach a maximum value. Energies above this optimum value cause no significant increase in atmosphere loss, while for smaller energies blow-off efficiencies decrease rapidly. Thus, for a given accretion rate and a given planet size most of the planetesimal sizes lie around a value giving rise to optimum energy levels for a then existing atmosphere, the dissipation effect of infalling bolides will reach its maximum. If a different size distribution prevails atmospheric loss via impact will be less efficient.

A major goal of the present study is the definition of boundary conditions, which will lead to either atmospheric growth during accretion or to atmospheric dissipation as a result of planetesimal infall. In the following, we will describe our numerical and model techniques. We will present model results and will discuss implications for the formation of impact-generated atmospheres on Venus, Earth and Mars.

2.0 NUMERICAL AND MODELLING TECHNIQUES

2.1 General

We model the formation of the planets and the growth of an impact-generated atmosphere in the framework of a Safronov-type accretion model. Once infall velocities of planetesimals exceed critical velocities for incipient to complete loss of structural water in water-bearing minerals, water vapor is added to an evolving proto atmosphere. At that point we consider the effect of bolide-atmosphere interactions in subsequent time steps of the model. We take the current mass of this atmosphere and its mean temperature into account to derive the relevant parameters (surface pressure, surface density) for the blow-off calculations. In our numerical modelling scheme, at the end of each iteration the evolving mass budget of the atmosphere (i.e., impact-induced minus blow-off) is obtained and is used as initial conditions for the following time step.

2.2 Accretion Model

The accretion rate, $\dot{m}$, assumed is that specified by (Safronov, 1972):

$$\dot{m} = \pi r^2 (1 + 2\theta) \rho_p u \tag{1}$$

where r is the current radius of the solid proto-planet, θ the Safronov-parameter, ρ_p the spatial density of planetesimals in the region of the growing planet and, u, the approach velocity or the velocity relative to the orbiting velocity of the planetesimals. Equation (1) can be transposed into:

$$\dot{m} = \pi r^2 (1 + 2\theta) \frac{4[M - m(t)]}{P_K \pi (a_0^2 - a_i^2)} \tag{2}$$

Thus M is the final mass of the planet, P_K it Keplerian period and a_0 and a_i are the radii of outer and inner edges of the feeding zone of planetesimals forming each planet (Safronov, 1972; Lange and Ahrens, 1986) (See Table I for the above values for the terrestrial planets).

Equation (2) is numerically solved and the time dependent mass, radius and fractional mass $f(t) = m(t)/M$ is obtained. The (constant) mean radius of planetesimals r_{pl} determines the number of planetesimals n_{pl} for each time step during accretion:

$$n_{pl}(t) = \frac{\dot{m}(t)}{(4/3)\,\pi r_{pl}^3 \bar{\rho}_{pl}} \tag{3}$$

where $\bar{\rho}_{pl}$ is the mean density of infalling planetesimals (assumed for simplicity to be equal to the final mean density of the planet).

For each iteration, the current surface gravitational acceleration $g(t)$ and escape velocity $V_e(t)$ are computed:

$$g(t) = G \frac{m(t)}{(r(t))^2} \tag{4}$$

$$V_e(t) = \sqrt{2 g(t) r(t)} \tag{5}$$

where $m(t)$ and $r(t)$ are the mass and radius of the planet and G the gravitational constant. Figure 1 gives $f(t)$ as a function of time for Venus, Earth and Mars.

2.3 Shock-induced Volatile Loss

Impacts of volatile bearing planetesimals upon volatile containing planetary protocrusts will cause degassing of both impactor and target provided, the shock pressures in each medium exceed critical pressures needed for incipient (P_{iv}) to complete (P_{cv}) shock-induced devolatilization (Lange and Ahrens 1982a). These critical pressures have been experimentally determined for serpentine (Lange and Ahrens, 1982a,b), brucite (Lange and Ahrens, 1984) and calcite (Lange and Ahrens, 1986). In the present study we consider only dehydration of serpentine as the major source of atmospheric gases, for which $P_{iv} = 12GPa$ and $P_{cv} = 33GPa$ (Tyburczy et al., 1986).

Assuming that planetesimal composition is approximated in composition and shock impedance by the impacted surface material, the peak initial shock pressure P is given by:

$$P = \bar{\rho}_{pl} (V_e/2) \; [C_o + S V_e/2] \tag{6}$$

We further assume that the impact velocities can be approximated by the escape velocity of the planet. $C_0 (= 3750 m/s)$ and $s (= 1.6)$ are equation of state parameters for pyroxene-bearing serpentinite as given by Marsh [1980]. Thus we effectively are using the equation of state of serpentinite centered at the mean density of the planet and planetesimals. These are all very simplistic assumptions.

We now consider only release of water from infalling planetesimals and neglect the contribution from shocked partially hydrous surface materials. Our previous studies have shown (Lange and Ahrens, 1982a,b, 1984) that redistribution and reactions of free atmo-

spheric water with surface minerals and metallic iron are probably not significant for the latter parts of the accretion process if the more iron-rich material accreted first. Thus we consider the build-up of a primary water atmosphere and its possible impact erosion occurring after the point where the planet has reached this point and f has achieved a value exceeding f_{bo}. We assume $f_{bo} = 0.75$ for most of our models based on our previous studies (Lange and Ahrens, 1982a,b, 1984) but also consider values in the range $0 \leq f_{bo} \leq 0.9$. The assumtion; $f_{bo} > 0.75$ implies that during the earlier parts of the accretion process most of the delivered and shock-released water will not reside in a proto atmosphere (cf. Jakosky and Ahrens, 1979).

We assume the amount of shock-induced water release dm for a given impact is obtained by:

$$dm_a = \begin{cases} 0 & \text{for } P < P_{iv} \\ m_{pl}\, f_w \quad [(P - P_{iv})\,/\,(P_{cv} - P)] & \text{for } P_{iv} \leq P \leq P_{cv} \\ m_{pl}\, f_w & \text{for } P > P_{cv} \end{cases} \tag{7}$$

where m_{pl} is the planetesimal mass, $\frac{4}{3}\pi r_{pl}^3$, and f_w the mass fraction of structurally bound water within the planetesimals. We assume $f_w = 0.01$ (Lange & Ahrens, 1984).

The mass of the water atmosphere at one particular time step without considering atmospheric crater $A'(t)$ is:

$$M_a'(t) = M_a'(t - \Delta t) + dm_a \tag{8}$$

where $M_a'(t - \Delta t)$ is the atmospheric mass at the preceding time step. The time step Δt we used was 10^6 years and a total accretion history of up to 10^8 years (Figure 1).

2.4 Surface Conditions and Atmospheric Properties

The conditions of the surface of the growing planet (e.g. its temperature) and atmospheric surface pressure and atmospheric scale height are closely coupled with and dependent on the amount of atmospheric gases M_a present.

In order to determine surface temperatures, we used two different approaches. In most of our models, surface temperatures were assumed to be constant and to equal a lower estimate for the solidus temperature at $P_S = P_{H_2O}(= 800K)$, where P_S is the atmospheric surface pressure and P_{H_2O} is the partial pressure of water at the surface (Abe and Matsui, 1984, Fricker and Reynolds, 1968).

As a second approach we assumed the evolving water atmosphere to be in radiative equilibrium. Under these conditions, the surface temperature T_S can be estimated by (Goody and Walker, 1972):

$$T_S = T_e(OT + 1)^{1/4} \tag{9}$$

here, T_e is the black body equilibrium temperature at the top of the atmosphere for a planet heated by solar radiation alone (Table I) and OT is the optical thickness or optical depth of the atmosphere, which is obtained by:

$$OT = \kappa_0 P_S / g \tag{10}$$

where κ_0 is the optical constant $(= 0.001 m^2/kg)$, g the gravitational acceleration (equation (4)) and P_S the surface pressure, which is:

$$P_S = M_a g / A_p \tag{11}$$

where $A_p = 4\pi r_p^2$ is the current surface area of the accreting planet and the M_a the present mass of atmospheric gases (see below).

The atmospheric scale height Δ is:

$$\Delta = T_S \cdot R / (g \bar{m}) \tag{12}$$

where R is the gas constant and $\bar{m}$ is the mean molecular weight of the atmosphere (18 for water).

The surface density ρ_S of the atmosphere is:

$$\rho_S = P_S \bar{m} / (R T_S) \tag{13}$$

2.5 Atmospheric Cratering

We apply the formalism of Bach et al. (1975) for explosive-induced blast waves in exponential atmospheres in order to approximate the effect of the interaction of the impact ejecta with the atmosphere. We assume this acts like an explosion at the solid planet - atmosphere interface. We use dimensionless variables, which specify in spatial coordinates, radius, r and angle, θ, from the vertical in an axisymmetric spherical coordinate system, the pressure and particle velocities at the shock front of the expanding blast wave as a function of time (see Ahrens & O'Keefe, 1987, fig. 22).

We assume a polytropic constant $\gamma(= 1.4)$ and use the particle velocity, u, normalized by the shock velocity w to define $f = u/w$. The non-dimensional source density $g = \rho_c \,/\, \rho_s$ is given as a function of the normalized radius coordinate $x = r/R_S$. Here ρ_c is the density at the source. We assumed a normalized characteristic dimension

$$\xi = R_S/\Delta \tag{14}$$

Here, R_S is the radius to the shock front of the expanding blast envelope. The solution of Bach et al (1975) we employ is derived from the solution of the non-dimensional, expanded form of the conservation equations for the Eulerian space profiles of a point-symmetrical blast wave by means of a perturbation technique. Here ω, the perturbation parameter, is defined as $\omega \equiv -d\ \ell n\, \rho_a/(d\ \ell n\, r)$ and the density ρ_a of the undisturbed atmosphere is given by:

$$\rho_a = \rho_c \exp\left(\frac{-R_S \cos\theta}{\Delta}\right) \tag{15}$$

and also $\omega = \xi \cos\theta$. Using these definitions, we can specify the dimensional values of u and ρ, for any value of x, given the initial values of particle velocity u_n and density ρ_c at the source of the explosion. For a strong shock in polytropic gas, the shock velocity w and particle velocity are simply related by

$$u_n \;=\; 2\,w\,/\,(\gamma + 1) \tag{16}$$

$$w = 4\,\Delta\,A \Big/ \left[\xi^{3/2} \exp\left(\omega\lambda_1/2 + \omega^2\lambda_2/4 + \omega^3\lambda_3/6\right)\right] \tag{17}$$

Here, A is a constant, related to the energy of the explosion, Eo, and the atmospheric scale height.

$$A = \left[E_O \Big/ \left(4\pi\,\Delta^5 \rho_s\, J_O\right)\right]^{1/2} \tag{18}$$

This constant, couples non-dimensional time $\tilde{t}$ with real time t:

$$\tilde{t} = t\,A \tag{19}$$

We assume that E_O, the energy of the explosion, equals the energy of the planetesimal which was partitioned into the atmosphere, and $\lambda_1, \lambda_2, \lambda_3, J_O$ are constants derived by Bach et al. (1975) for $\gamma = 1.4$.

Thus, specification of E_O (we assume $\sim 1/3$ of impactor energy is partitioned into atmosphere; O'Keefe and Ahrens, 1982) by:

$$E_O = (m_{pl}\, V_e^2)/6 \tag{20}$$

yields the value of A for a given scale height (eq. (18)) and atmospheric surface density (eq. (13)). Thus for a specific value of ω and ξ, we can determine the shock front velocity w (eq. (17)) and particle velocity u_n (eq. (16)). Finally, given ω and ξ (and hence via eq. (14) the shock front radius R_s), the values of u/u_n for an arbitrary value of x (and hence a

specific radial distance $r = xR_S$) yields the value of the particle velocity behind the shock front from the results of Bach et al., (1975). This procedure thus allows specification of particle velocities of zones in the immediate vicinity of the evolving shock front of the blast waves. In order to apply this theory at sufficiently high altitudes such that the gas mean free path is comparable to the zone dimensions, we use values of the velocity field parameters for which $\omega = 10$. Once these velocities exceed the escape velocity of the accreting planet V_e (eq. (5)), it is assumed that the atmospheric mass in the corresponding zone escapes the planet. In our calculations, we utilize a flat-Earth approximation. Ahrens and O'Keefe (1987) discuss some aspects of this approximation; however more effort needs to be expended on this question in the future.

In order to compute the mass in the zones within the expanding shock front, the density profiles as a function x and the density behind the shock were obtained from the values of ρ/ρ_s given by Bach et al, 1975.

The atmospheric density ρ_s at the shock front, for strong shocks is:

$$\rho_s = h\rho_a \tag{21}$$

where

$$h = (\lambda + 1) / (\lambda - 1) \tag{22}$$

where ρ_a is given by eq. (15).

We must also specify zone geometry in order to determine their mass content from their density and volume. This is done by considering quasi-spherical sectors (the shock envelope is not a sphere but an ellipsoid; see Fig. 22 of Ahrens and O'Keefe, 1987), where a twelve-fold radial- and a nine-fold angular spacing was assumed. This results in 108 zones, for each of which we determine gas particle velocity, gas density, zone volume, and zone mass. We assume that the atmospheric mass in those zones escapes from the planet only if the particle velocity is greater than the current escape velocity of the planet.

The sum of these masses determines the mass of M_a blown-off atmosphere, $M_{al}(t)$, while the difference between the amount of gas delivered by the planetesimals and lost, M_{al} added to whatever atmospheric mass is present from the previous step, yields the current mass M_a of the proto-atmosphere. The cummulative amount of blown-off gas M_{cl} during the course of accretion determines the total mass of dissipated atmosphere at the end of the planetary formation process.

3.0 RESULTS AND DISCUSSION

The major results of our model studies for Earth, Venus, and Mars with model parameters given in Table II are discussed below. We varied three parameters, planetesimal radius r_{pl}, the mass fraction of the planet, at which atmospheric cratering began, f_{bo}, and the method by which we determined surface temperatures (see sect. 2.4). The choice of either a constant surface temperature T_s or a variable one, determines whether the blow-off process is coupled (via the scale height) to the mass of atmospheric gases present.

3.1 Earth

Figure 2 gives the time history of atmospheric evolution for models with constant planetesimal radius of 90 km. Panel (a) shows the situation for a model with constant surface temperature and model (b) depicts the evolution, which involves a feedback between surface temperature and the amount of atmospheric gas present (which determines the optical thickness OT, equations (10) and (11)). As can be seen, upon initiation of atmospheric blow-off process (at $f(t) = f_{bo} = 0.75$), the mass of dissipated gas M_{al} reaches a maximum (at $\sim 1.58 \times 10^{15}$s). This is followed by a series of local maxima and minima in M_{al}, which reflects unsteady behavior resulting when the mass of atmospheric gases present, M_a and the amount of dissipated gas at the same time, are of approximately the same magnitude. Once, M_a becomes significantly larger than M_{al}, these oscillations in M_{al} disappear and a steady decrease in M_{al} is calculated. This is caused primarily by the fact that with f(t) approaching 1, the accretion rate $\dot{m}(t)$ and thus the number of planetesimals $n_{pl}(t)$ (equations (1-3)) and hence impactors has declined. Since most of the planet is formed at this time, the planetesimal infall velocities $V_e(t)$ stay almost

constant (because of nearly constant g(t); equations (4) and (5)) and the slight increase in planetesimal energies delivered to the atmosphere cannot counterbalance the effect of decreasing planetesimal numbers (Figure 3).

This decrease in M_{al}(t) is somewhat more pronounced for model (b), resulting in less efficient impact cratering of atmospheric gases and a smaller value of the cumulative mass of blown-off gas M_{cl} at the end of accretion. This results from the higher surface temperatures T_s in this model compared to the constant value of T_s = 800K in model (a). While for the latter model the scale height Δ remains at an approximately constant value of 38 km, Δ values in model (b) are higher and vary significantly with time (Figure 4). As can be seen in fig. 4, due to the increase in atmospheric mass M_a, which is reflected in the increase in surface pressure P_s and surface density ρ_s, the optical depth OT and thus surface temperatures T_s increase correspondingly (equations (9-13). This leads to an increase in atmospheric scale height Δ, which leads to *decreased* efficiencies of the atmospheric cratering process, mainly because of lower atmospheric densities ρ_a for a given height (equation (15)).

Figure 5 summarizes the model study for Earth. The optimum planetesimal radius (which we define as r^*_{pl} in the following:) is that planetesimal size, which results in the maximum value of $M_{cl}(\tau)$, the cumulative mass of impact-dissipated gas by the end of accretion (see also Table II). This quantity increases very slowly with increasing planetesimal radius for $r_{pl} \lesssim 15$ km. At that point, blow-off efficiencies increase dramatically with increasing r_{pl}, until the optimum value r^*_{pl} is reached. From this point on, $M_{cl}(\tau)$ decreases steadily with increasing r_{pl}, but at a slower rate than seen in the rising part of

the curve.

This result parallels the findings of Ahrens and O'Keefe (1987). They show that for small impactor energies (or impactor sizes) impact cratering atmosphere loss (blow-off) efficiencies are very small and become zero below a critical minimum energy. They also show that upon reaching maximum efficiencies, blow-off rates remain constant with increasing impactor energies. This, in conjunction with the decreasing planetesimal number as a function of size for a given accretion rate leads to the observed decrease in M_{cl} for $r_{pl} > r^*_{pl}$. Thus, while the increase in impactor energy does not influence blow-off rates, the decrease in planetesimal number leads to a decreasing cumulative efficiency of the atmospheric cratering processes.

As can be seen (fig. 5), the choice of either constant or variable surface temperatures affects both, the value of r^*_{pl} as well as the maximum value of M_{cl}, as discussed above (Table II). (Subsequently, we will concentrate on models with variable T_s, because they are probably more realistic.)

Shock-induced water release in infalling planetesimals starts, when the accreting planets are still small. For Earth and Venus, this point lies at $f \simeq 0.016$ (Tyburczy et al., 1986). If we assume that timescales for processes, which consume atmospheric water, i.e. readsorbtion of water by anhydrous minerals (Jakosky and Ahrens, 1979) and iron water reactions (Lange and Ahrens, 1984) require longer timescales than atmospheric cratering events (i.e. essentially the timespan between subsequent planetesimal infalls), then atmospheric blow-off could be important in the earlier stages of accretion as well. In order to explore this situation, we conducted a series of calculations, where we varied f_{bo} between

0.001 and 0.9 (Table II). For these models, we used the optimum planetesimal radius r^*_{pl} (figure 5) for the case of variable surface temperatures. Figure 6 gives the final values of M_a and M_{cl} as a function of f_{bo}. As can be seen, for small values of f_{bo}, i.e. for models in which dehydration and blow-off is considered for earlier phases of the accretion process, the amount of atmospheric gases greatly exceeds the cumulative amount of blown-off gas (by up to a few orders of magnitude). This is due to the fact that while infall energies are sufficient for shock-induced release of structural water, the fraction of this energy partitioned into the evolving atmosphere does not lead to appropriate blow-off efficiencies.

The larger f_{bo} becomes, the smaller the difference between M_a and M_{cl} gets, until from about $f_{bo} \sim 0.65$, the curves are approximately parallel. For $f_{bo} \rightarrow 1.0$, both curves will approach 0. Thus, it can be seen (fig. 5 and fig. 6) that atmospheric cratering is insufficient to completely remove an evolving proto-atmosphere, at least in the flat-planet approximation.

3.2 Venus

Several features of our models for Venus are similar to those of the Earth, which are depicted in figures 2 and 3. Figure 7, gives atmospheric surface properties for Venus. Because of the higher effective temperature T_e (Table I), surface temperatures are higher than on Earth. This results in a greater atmospheric scale height. Since $r^*_{pl} = 130$ km (fig. 8), the results shown represent the minimum feedback between surface temperature and mass of atmosphere present, i.e. for less or greater values of r_{pl}, surface temperatures will be higher because of larger resulting values of M_a. Greater masses of atmospheric

gases lead to higher surface temperatures and subsequently greater scale heights (equations 9-12). Also, greater scale heights result in decreased blow-off efficiencies.

Cumulative blow-off efficiencies as a function of radius are given in Figure 8. As can be seen, the optimum planetesimal size r^*_{pl} for variable surface temperatures lies at $\sim$ 130 km as compared to $\sim$ 100 km for Earth. Other properties of both M_{cl} and M_a as a function of r_{pl} are similar, except for a slightly larger shift to low values for the optimum planetesimal radius in the case of constant surface temperatures (cf. Table II).

The difference between r^*_{pl} for Earth and Venus (the Earth is characterized by only slightly larger mass and mean density compared to Venus) can be explained in terms of two effects. Because of its smaller mass and smaller mean density, planetesimal infall velocities are slightly lower for Venus and the amount of energy partitioned into the atmosphere significantly lower than on Earth for a given planetesimal size. Secondly, due to higher equilibrium temperatures, surface temperatures on Venus are higher and consequently the greater atmospheric scale height implies that in order to reach similar blow-off rates, Venus-planetesimals need to be larger than those accreting on Earth. Hence, both effects call for larger planetesimal sizes to obtain comparable blow-off efficiencies on Venus and probably explain the higher value of r^*_{pl} on Venus as compared to Earth.

As on Earth, it can be seen that atmospheric cratering does not accelerate to escape velocities all of the evolving atmospheric gases. Thus, the present class of models predict that on Venus a more substantial proto-water atmosphere was present by the end of accretion than for the Earth.

Figure 9 gives the final amounts of atmospheric gas as well as the total amount of

blow-off atmosphere as a function of f_{bo} (cf. figure 6). As can be seen, similar to the results obtained for Earth, a different choice of f_{bo} as that used for the models of figure 8, does not result in more efficient atmospheric cratering by infalling plantesimals.

3.3 Mars

Mars, because it is a smaller planet demonstrates a smaller range of T_s, Δ and P_S than the other terrestrial planets during the atmospheric accretion process. For Mars, we find $r^*_{pl} = 160$ km (fig. 11). Atmospheric mass M_a remains less for Mars than for Earth and Venus during accretion mainly because of the smaller value of g. This in-turn increases OT for a given surface pressure P_S. However the resultant surface temperatures on Mars are similar to those on the larger planets (Figure 10), but the smaller value of g results in significantly larger values of Δ and lower values for P_S for Mars as compared to Venus and Earth.

As for Venus, the lower value of g in conjunction with an enlarged atmospheric scale height is the reason for an again increased value of r^*_{pl} for Mars as compared to Earth and Venus (Figure 11). Both factors require larger planetesimal sizes to obtain blow-off rates on Mars, comparable to Earth, and Venus.

In contrast to the other planets, the cumulative mass of blown-off gas for the optimum plantesimal exceeds the amount of atmospheric gas present. However, there is still some atmosphere present at the end of accretion. Thus, on Mars, planetary cratering appears to be so effective that a large fraction of the volatiles delivered to the planet during accretion was lost for planetesimal radii being equal to r^*_{pl}. Other aspects of M_a and M_{cl} versus r_{pl}

are similar for the three planets, particularly the shift to a smaller value of r^*_{pl} for models with constant surface temperature and a decrease in M_a / M_{cl}. We will now define the ratio M^*_{cl} as the value of M_a / M_{cl} at $r_{pl} = r^*_{pl}$.

Figure 12 gives M_a and M_{cl} as a function of f_{bo} for r_{pl} = 160 km (starting at f_{bo} = 0.1, as discussed above). Similar to the results of figure 11, it can be seen that for 0.66 $\lesssim f_{bo} \lesssim$ 0.85 the value of the functions, M_{cl}, actually exceeds M_a. Thus, for models, which treat atmospheric blow-off from planets with large values of f_{bo}, the total rate of atmospheric loss by cratering exceeds the rate of gas which is delivered to the planet. As a result, for $f_{bo} \rightarrow 1$, both M_a and M_{cl} will approach zero.

4.0 CONCLUSIONS

Atmospheric cratering and the associated loss of of atmospheric gases to space has a significant effect on the evolution of a primary, impact-induced atmosphere on the terrestrial planets. Once the mean planetesimal size exceeds a critical lower limit (~15, ~25 km and ~30 km for Earth, Venus, and Mars, respectively), total blow-off efficiencies become significant, rapidly reaching 5 to 10% of the final atmosphere with each accretional increase to the atmosphere. Accretion of an H_2O atmosphere by planetesimals with radii greater than about 40 km will at the same time suffice to yield a total water loss equal to one Earth-ocean mass.

Abe and Matsui (1985, 1986) and Matsui and Abe (1986) have shown, that the early H_2O rich atmosphere proposed by Lange and Ahrens (1982a,b) will as a result of thermal blanketing rapidly form a global magma ocean of unspecified depth on the accreting ter-

restrial planets. Moreover the amount of water in the atmosphere will be transferrred to the molten layer by the solubility of water in the magma. They further show that plausible models will lead to a final amount of free water approximately equal to one ocean mass. However some degree of inhomogeneous accretion must have occurred, to both inhibit the water-iron reactions and to allow the low value Fe/(Fe + MgO) ratio in the Mars, Venus, and Earth mantle, compared to cosmic abundance, to be achieved (Lange and Ahrens, 1984, Ringwood, 1977).

Our results imply that the atmospheric cratering must be considered in future atmospheric accretion models as large amounts of atmospheric water vapor on the Earth and the other planets could have been easily dissipated by blow-off processes. As a consequence, the Abe and Matsui, (1985, 1986); Matsui and Abe (1986) result, in which they obtained the present H_2O budget for the Earth with their accretion scenarios appears to be fortuitious. However we believe this application of the early ideas of Ingersoll (1969) and Rasool and De Bergh (1970) to atmospheric evolution has been valuable.

Blow-off efficiencies depend critically on the radius of the infalling objects. Thus the question arises, what are realistic planetesimal radii for the latter part of the accretion of the terrestrial planets? There is little direct evidence, which could shed light on this question, but theoretical considerations suggest that larger planetesimal sizes ($r_{pl} \sim 10^2$ to 10^3 km) dominated the size distribution in the last accretional stages (Wetherhill, 1985). Thus, we conclude that the sizes of our optimum planetesimal radii, r^*_{pls} fall within this range. The effects of even larger impactors on proto-atmospheres also need to be studied via other methods. Moreover, instead of a constant fraction of energy coupling into the

atmosphere the plan size distribution, covering a large range of radii and impact velocity requires study.

Figure 13 summarizes the regimes of the terrestrial planets and the present results. Shown are the final mass of the planet M, the effective equilibrium temperature T_e, the optimum planetesimal radius r^*_{pl} and the ratio M_a / M_{cl} evaluated at $r_{pl} = r^*_{pl}$ or, M^*_{cl} as a function of mean distance from the sun for Venus, Earth, and Mars. While T_e mainly influences the surface temperature T_s and thus the scale height Δ, the planetary mass determines primarily the infall velocity of the planetesimals. The latter will strongly affect the amount of energy available for partitioning into the atmosphere and thus the efficiency of atmospheric blow off for a given planetesimal size. Thus, one would expect the maximum blow-off efficiency, M^*_{cl}, to be reached at the optimum planetesimal radii, r^*_{pl}, inversely proportional to planetary mass, M. This is seen in figure 13.

The amount of gas ejected from a planetary atmosphere upon impact also depends on the density structure of the atmosphere and thus on Δ. With increasing Δ, the amount of gas blow-ff for a given impact should decrease. Thus, one would expect to see an inverse dependence of M_{cl} on Δ. This is transposed into an approximate proportionality between T_e (increasing T_e lead to increasing Δ) and M^*_{cl} (increasing Δ result in <u>*decreasing*</u> M_{cl} and in increasing M^*_{cl}), as seen in figure 13.

Finally, our results demonstrate that atmospheric cratering gas loss, regardless of whatever choice of boundary conditions is taken, will <u>*not*</u> suffice to completely dissipate a primary atmosphere of a gas with an intermediate molecular weight (18) such as water on Earth and Venus. Mars, however, may have suffered an almost complete loss of a primary

atmosphere because of atmospheric cratering losses. Thus, we conclude that a primary, impact-induced atmosphere remains a realistic option for Earth and Venus and is less likely for Mars.

Acknowledgements: Supported under NASA Grant NGL-05-002-105 and NSG-7129. We are grateful to the organizers of the Conference on Origin and Evolution of Planetary and Satellite Atmospheres, Tucson, AZ, March 1987, for an opportunity to present this work to an interested and critical audience. M.A. Lange's major support is derived from the A.-Wegener-Institute for Polar and Marine Research, Bremerhaven. Contribution No. 4508, Division of Geologic- al and Planetary Sciences, California Institute of Technology, Pasadena, CA 91125.

REFERENCES

Abe, Y. and T. Matsui, (1985). The formation of an impact-generated H_2O atmosphere and its implications for the early thermal history of the Earth. In Proc. Lunar Sci. Conf. 15th, Part 2, J. Geophys. Res., C545-559.

Abe, H. and M. Matsui, (1986). Early evolution of the Earth: Accretion, atmospheric formation, and thermal history. In Proc. Lunar Sci. Conf. XVII, Part I, J. Geophys. Res., 91, E291-E302.

Ahrens, T. J. and D. J. O'Keefe (1987). Impact on the Earth, ocean, and atmosphere. In Proc. Hypervelocity Impact Symposium, Int. J. Impact Engineering, 5, 13-32.

Ahrens, T.J., J.D. O'Keefe, and M.A. Lange, (1987). Formation of planetary atmospheres during accretion. In Origin and Evolution of Planetary and Satellite Atmospheres, ed. by S.K. Atreya, J.B. Pollak and M.S. Mathews, Univ. of Ariz. Press, in press.

Bach, G. G., A. L. Kuhl, and A. K. Oppenheim (1975). On blast waves in exponential atmospheres. J. Fluid Mech. 71 (1), 105-122.

Cameron, A.G.W., (1983). Origin of the atmospheres of the terrestrial planets. Icarus, 56, 195-201.

Fricker, P.E. and R.T. Reynolds, (1968). Development of the atmosphere of Venus. Icarus, 9, 221-230.

Goody, R. M. and C. G. Walker (1972). Atmospheres., Prentice-Hall, Inc., 150 pp.

Ingersoll, A.P., (1969). The runaway greenhouse: A history of water on Venus? J. Atmos. Science, 26, 1191-1198.

Jakosky, B. M. and T. J. Ahrens (1979). The history of an atmosphere of impact origin. Proc. Lunar Planet. Sci. Conf. 10th, 2727-2739.

Lange, M. A. and T. J. Ahrens (1982a). The evolution of an impact-generated atmosphere. Icarus 51, 96-120.

Lange, M. A. and T. J. Ahrens (1982b). Impact-induced dehydration of serpentine and the evolution of planetary atmospheres. Proc. Lunar Planet. Sci. Conf. 13th (1), J. Geophys. Res. 87 (suppl.) A451-A456.

Lange, M. A. and T. J. Ahrens (1984). FeO and H_2O and the homogeneous accretion of the Earth. Earth Planet. Sci. Lett., 71, 111-119.

Lange, M. A. and T. J. Ahrens (1986). Shock-induced CO_2 loss from $CaCO_3$: implications for early planetary atmospheres. Earth Planet. Sci. Lett., 77, 409-418.

Lange, M. A. and T. J. Ahrens (1987). Accretion of the icy Jovian and Saturnian satellites. To be submitted to ICARUS.

Marsh, S. P. (1980). LASL Shock Hugoniot Data. Univ. of California Press, Berkeley, CA., 680 pp.

Matsui, T. and Y. Abe (1986). Evolution of an impact-induced atmosphere and magma ocean on the accreting Earth, Nature, 319 (6051), 303-305.

O'Keefe, J. D. and T J. Ahrens (1982). The interaction of the Cretaceous-Tertiary extinction bolide with the atmosphere, ocean, and solid earth, in Geological Implications of Impacts of Large Asteroids and Comets on the Earth, Geol. Soc. Amer. Spec. Pap., 190, Boulder, Colorado, 103-120.

Rasool, S.I. and C. De Bergh, (1970). The runaway greenhouse and the accumulation of CO_2 in the Venus atmosphere. In Nature, 226, 1037-1039.

Ringwood, A. E. (1979). Origin of the Earth and Moon. Springer-Verlag, New York, Berlin.

Safronov, V. S. (1972). Evolution of the Protoplanetary Cloud and Formation of the Earth and Planets. NASA-TT-F-667.

Tyburczy, J. A., B. Frisch, and T J. Ahrens (1986). Shock-induced volatile loss from a carbonaceous chondrite: implications for planetary accretion. Earth Planet. Sci. Conf., 80, 201-207.

Wetherhill, G.W., (1985). Occurance of giant impacts during the growth of the terrestrial planets, Science, 228, 877-879.

Zel'dovich, Y. B. and Y. P. Raizer (1967). Physics of Shock Waves and High Temperature Hydrodynamic Phenomena. Academic Press, New York.

Table I: Physical Parameters for Terrestrial Planets

Planet	M, (kg)	R, m	$\bar{\rho}, kg\,m^{-3}$	C_A, m^2	f_w	T_e, K
Venus	4.87×10^{24}	6.05×10^{6}	5.27×10^{3}	3.05×10^{22}	0.01	320
Earth	5.97×10^{24}	6.38×10^{6}	5.52×10^{3}	5.98×10^{22}	0.01	253
Mars	6.42×10^{23}	3.40×10^{6}	3.95×10^{3}	1.12×10^{23}	0.01	210

M = Mass; R = radius; $\bar{\rho}$ = mean (compressed) density;
P_K = Kepleian period
$C_A = \pi(a_0^2 - a_1^2)$, a_0, a_i = radii of outer and inner feeding zones upon accretion; f_w = mass fraction of water in planetesimals;
T_e = effective temperature of planet

Table II: Model Parameters and Results

Planet	Model No.	r_{pl}, km	f_{bo}	T_s, K	M_a Kg	Kg	M_{cl} Earth-Ocean Masses	$M_a / M_{cl} = M^*_{cl}$
VENUS	VE100-	10-	0.75	variable[1)]	1.2×10^{22}	4.5×10^{20}	0.3	26.4
	VE109	200			7.9×10^{21}	4.3×10^{21}	3.2	1.8
	VE200-	70-	0.75	800	7.2×10^{21}	5.0×10^{21}	3.7	1.4
	VE203	130			7.8×10^{21}	4.4×10^{21}	3.3	1.8
	VE300-	130	0.0	variable[1)]	4.8×10^{22}	3.9×10^{19}	0.03	1231
	VE305		0.9		3.4×10^{21}	1.7×10^{21}	1.2	2.0
EARTH	EA100-	10-	0.75	variable[1)]	1.5×10^{22}	1.9×10^{20}	0.1	78.9
	EA115	600			1.3×10^{22}	2.2×10^{21}	1.6	5.9
	EA200-	1	0.75	800	1.5×10^{22}	1.9×10^{20}	0.1	78.9
	EA211	100			8.7×10^{21}	6.1×10^{21}	4.5	1.4
	EA300	90	0.0	variable[1)]	5.9×10^{22}	3.4×10^{19}	0.03	1735
	EA303		0.9		3.5×10^{21}	2.1×10^{21}	1.5	1.7
MARS	MA180	10	0.75	variable[1)]	1.8×10^{21}	9.4×10^{19}	0.07	19.1
	MA118	800			1.2×10^{21}	0.4×10^{20}	0.3	3.0
	MA200	80	0.75	800	8.4×10^{20}	8.1×10^{20}	0.6	1.0
	MA207	160			8.3×10^{20}	8.2×10^{20}	0.6	1.0
	MA300	160	0.1	variable[1)]	5.3×10^{21}	4.8×10^{20}	0.4	11.0
	MA305		0.9		3.4×10^{20}	3.0×10^{20}	0.2	1.1

1) T_s computed from equation (9).

(r_{pl} = planetesimal radius; f_{bo} = mass fraction of growing planet at which atmospheric cratering begins, T_s = surface temperature; M_a = mass of atmosphere; τ = accretion time; M_{al} = incremental mass of blown-off atmosphere)

FIGURE CAPTIONS

Figure 1. Assumed mass fraction f(t) of accreted planet versus time (years) for Venus, Earth, and Mars from Safronov accretion model.

Figure 2. Mass of atmospheric (M_a), mass of blown-off atmosphere (M_{al}) and cumulative mass of dissipated atmosphere (M_{cl}) as a function of time during the final part of Earth's accretion. Planetesimal radius, r_{pl}, used as 90 km. (a) constant surface temperature, 800 K. (b) radiative model.

Figure 3. Number of planetesimals, n_{pl}, planetesimal energy delivered to the atmosphere E_o, versus time for models with radii $r_{pl} = 10$ km (a) 100 km (b).

Figure 4. Earth surface temperature, T_s, atmospheric surface density ρ_s and scale height, Δ, versus time, planetesimal radius, r_{pl}, 100 km.

Figure 5. Mass of atmospheric gases, M_a, and cumulative mass of impact-ejected gas M_{cl} upon the accretion of the Earth as a function of planetesimal radii, r_{pl}. Plotted are results for constant surface temperature T_s (dashed curves) and radiative models (solid curves); $f_{bo} = 0.75$.

Figure 6. Mass of atmosphere M_a and final cumulative mass of blown-off gases M_{cl} as a function of the mass fraction f_{bo} at which atmospheric cratering processes first acts. Planetesimal radius, $r_{pl} = 100$ km.

Figure 7. Same as Figure 4, except for Venus, $r_{pl} = 130$ km.

Figure 8. Same as Figure 5, except for Venus.

Figure 9. Same as Figure 6, except for Venus and $r_{pl} = 130$ km.

Figure 10. Same as Figure 4, except for Mars, $r_{pl} = 160$ km.

Figure 11. Same as Figure 5, except for Mars.

Figure 12. Same as Figure 6, except for Mars and $r_{pl} = 160$ km.

Figure 13. Planetary mass M, equilibrium, radiation temperature T_e optimum planetesimal radius r^*_{pl} and the ratio between M_a and M_{cl} for $r_{pl} = r^*_{pl}$, M^*_{cl}, as a function of mean distance from the sun, for Venus, Earth, and Mars.

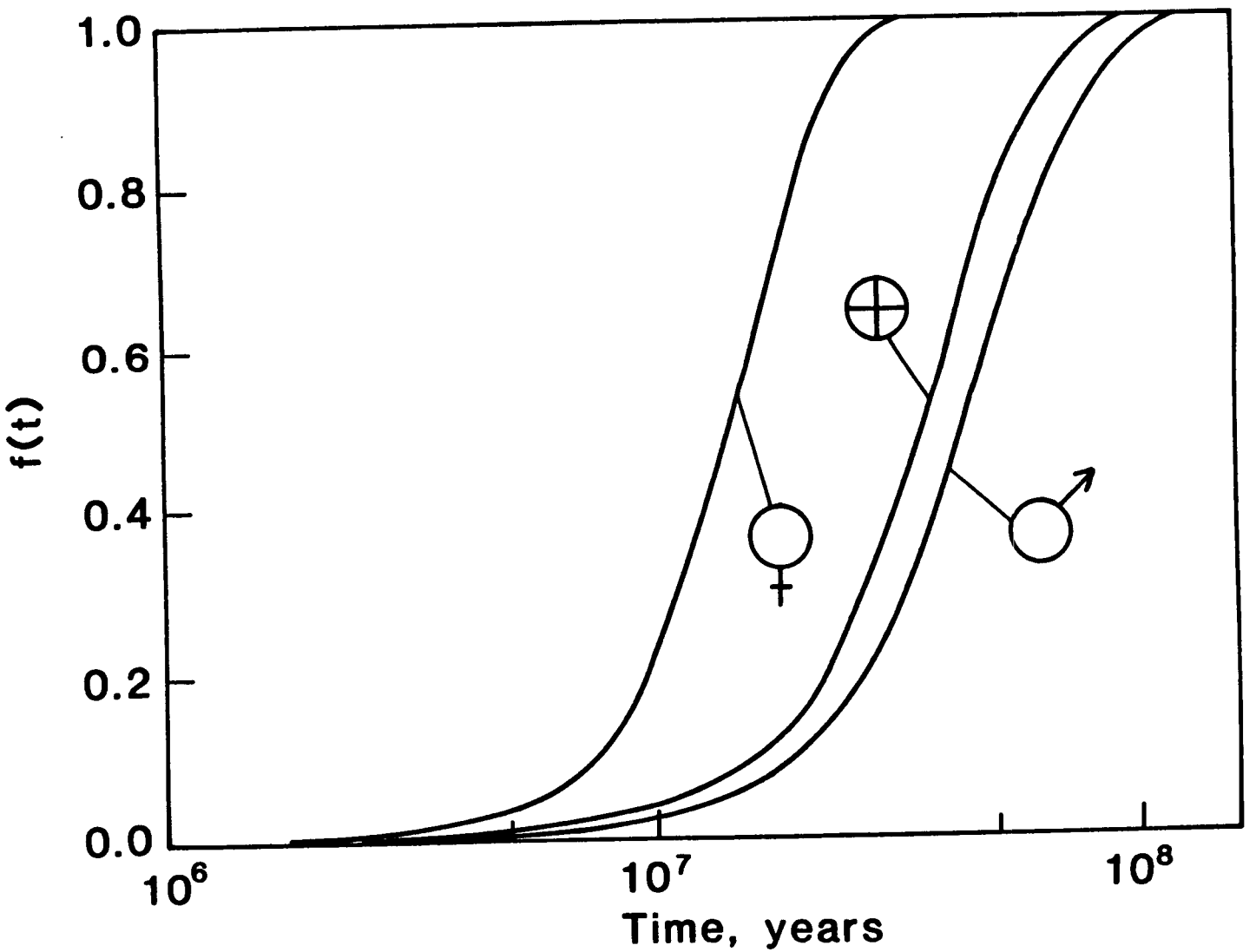

TJA87001SFD

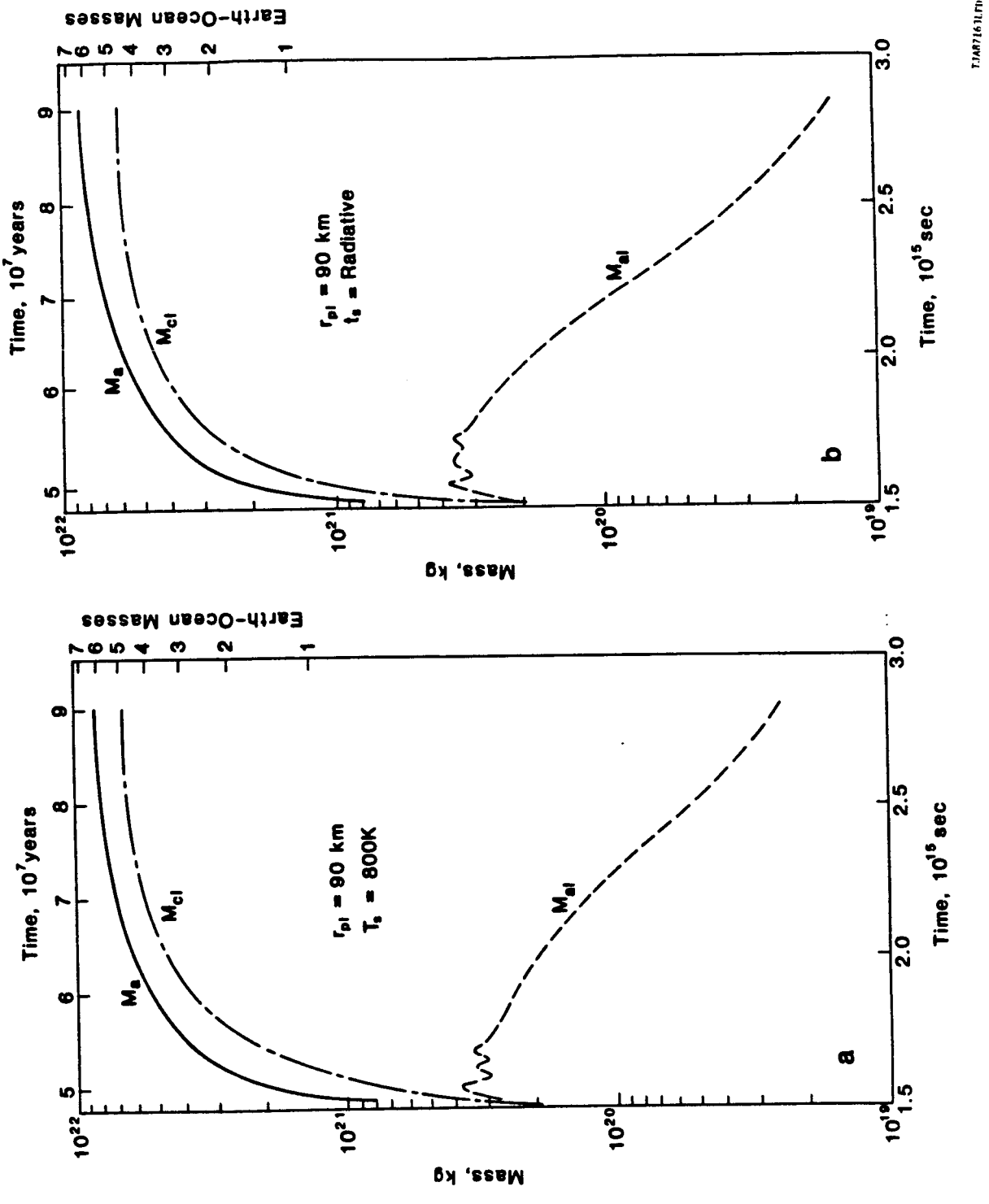
Earth-Ocean Masses
Time, 10^7 years
Mass, kg
Time, 10^{15} sec
M_s
M_{cl}
M_{al}
r_{pl} = 90 km
T_s = 800K
t_s = Radiative
a
b

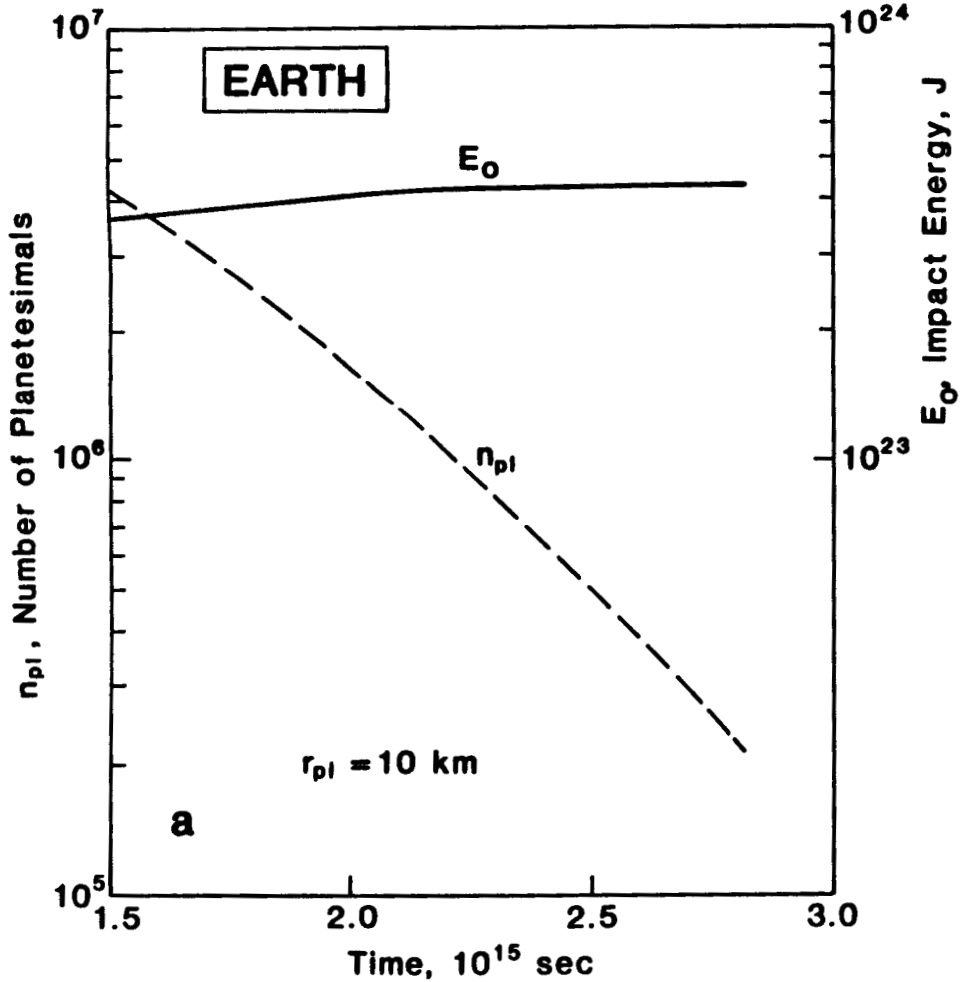

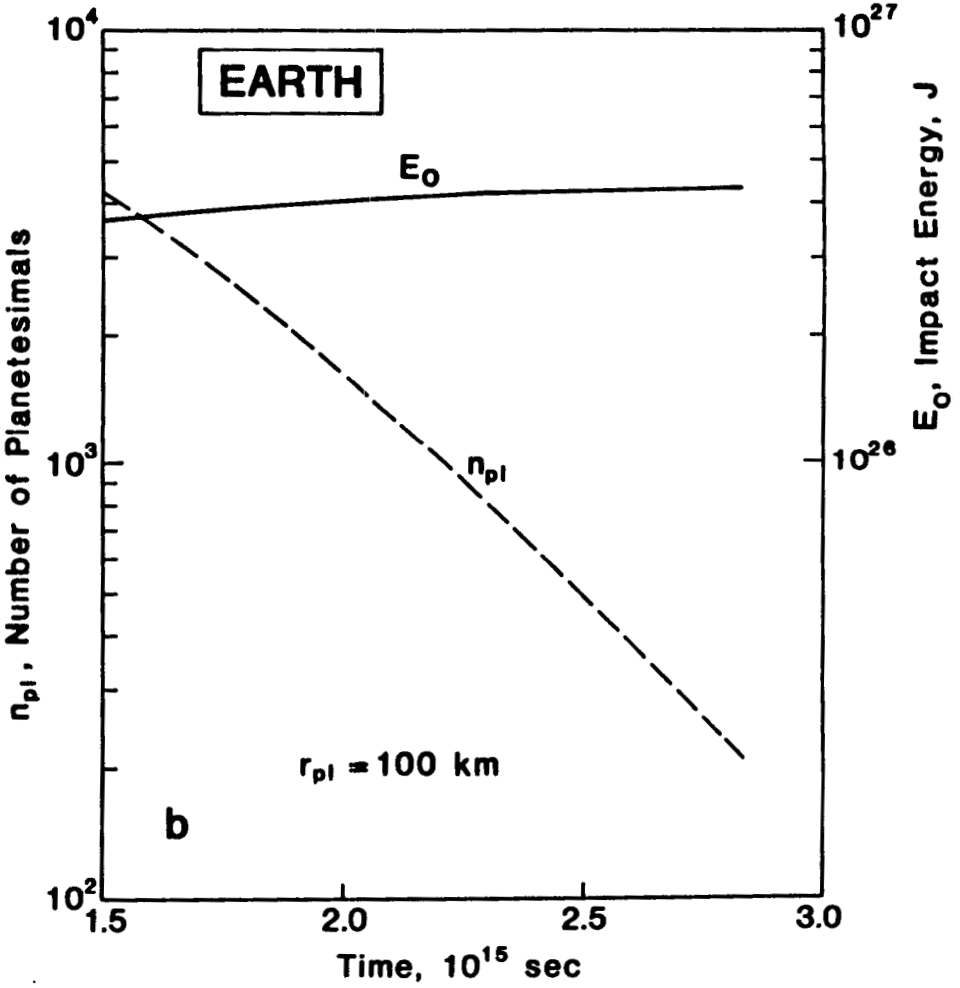

TJA88002LFD

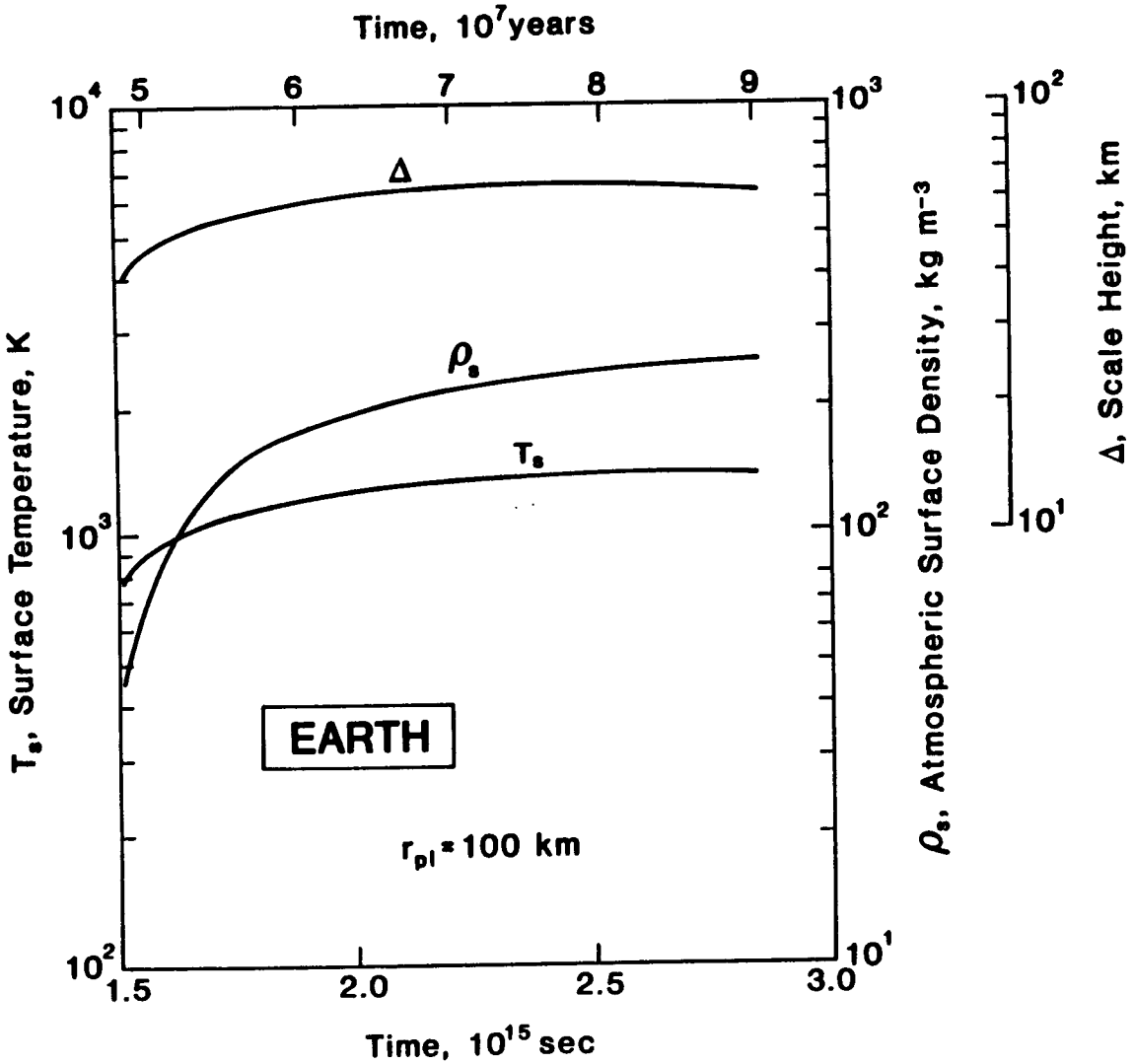
Time, 10^7 years
5
6
7
8
9
10^4
10^3
10^2
Δ
ρ_s
T_s
EARTH
r_{pl} = 100 km
1.5
2.0
2.5
3.0
Time, 10^{15} sec
T_s, Surface Temperature, K
10^3
10^2
10^1
ρ_s, Atmospheric Surface Density, kg m^{-3}
10^2
10^1
Δ, Scale Height, km

TJA87164SC

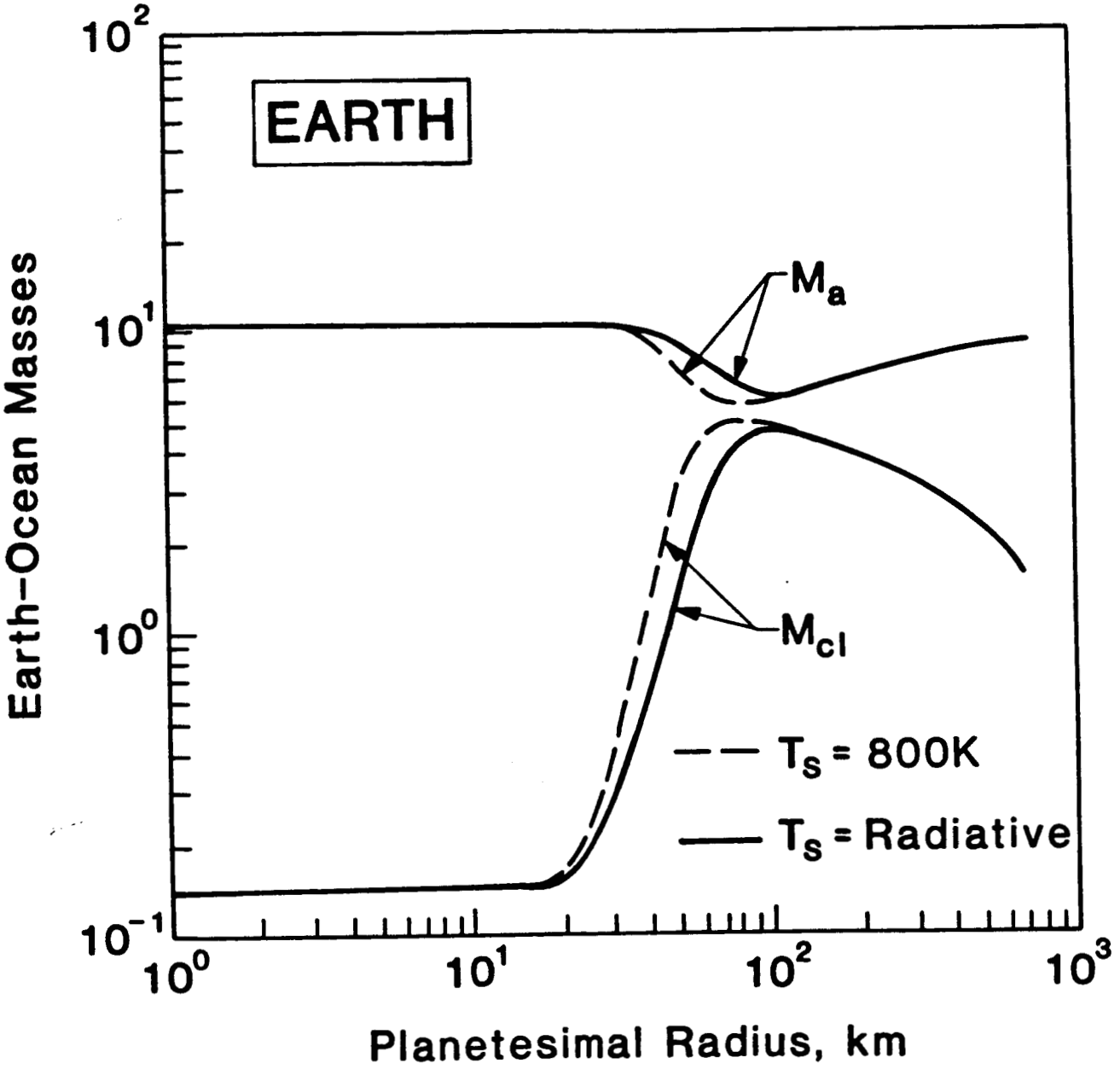

TJA87165SFD

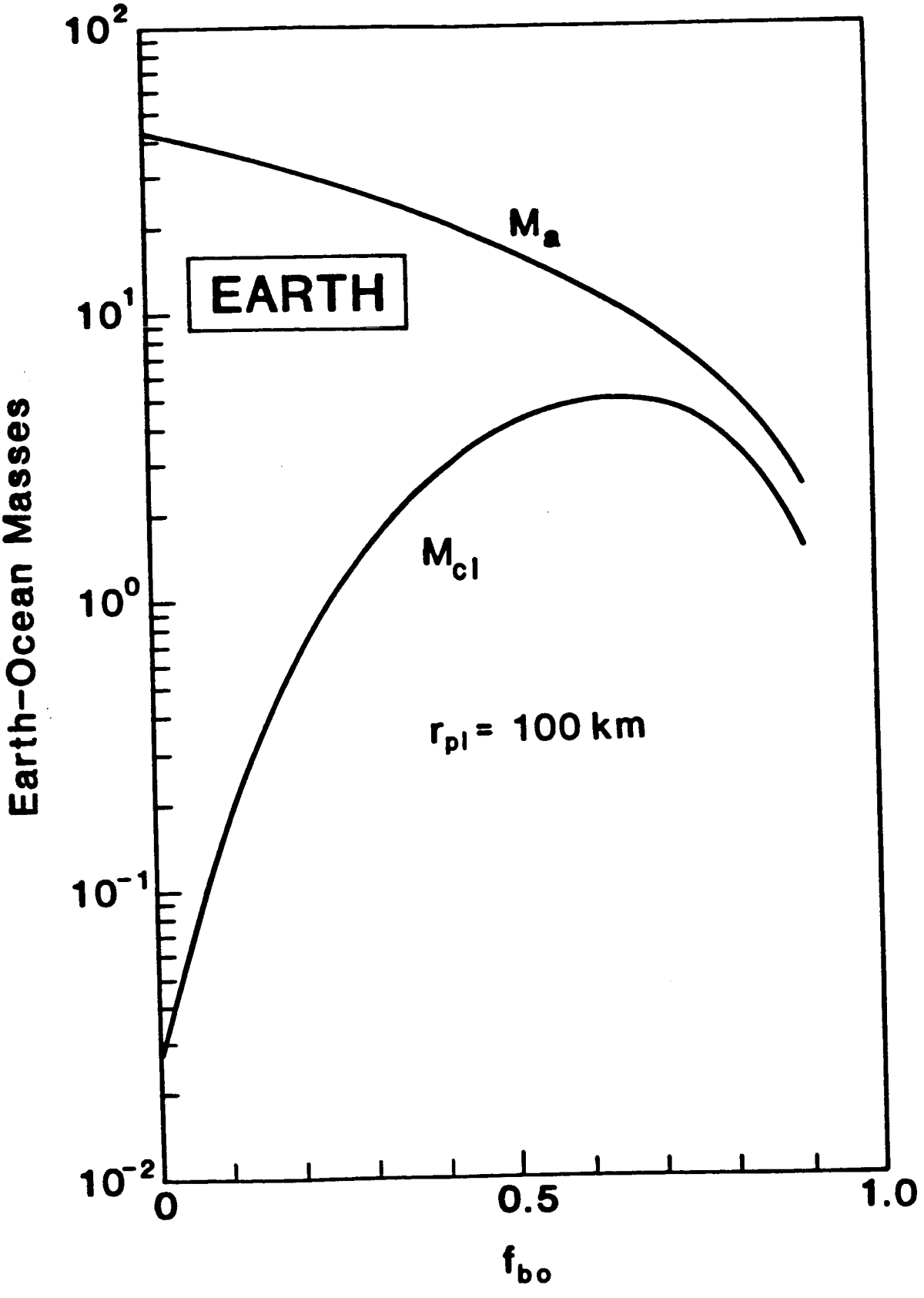

TJA87166SFD

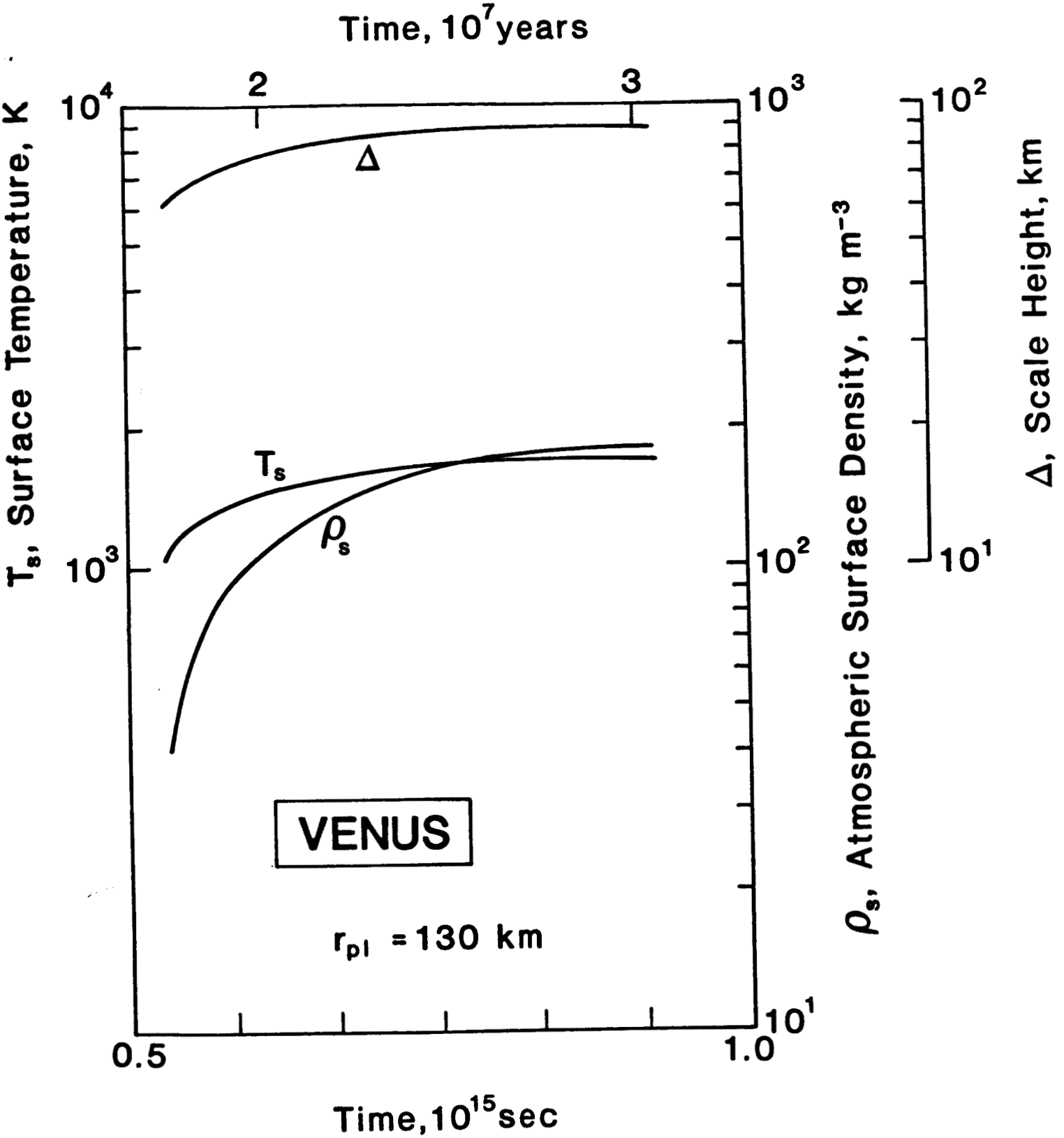

TJA87171SFD

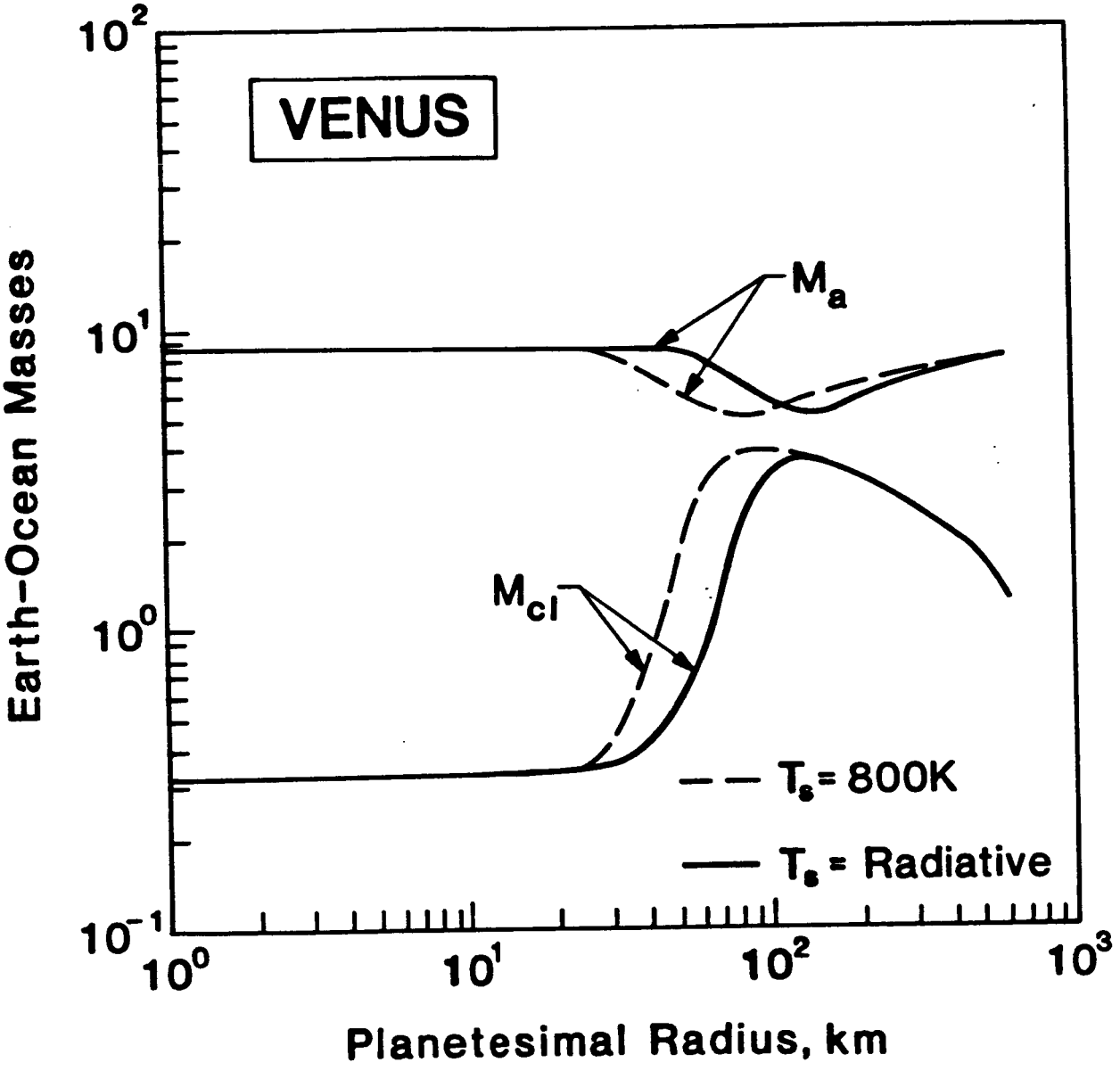

TJA88003SFD

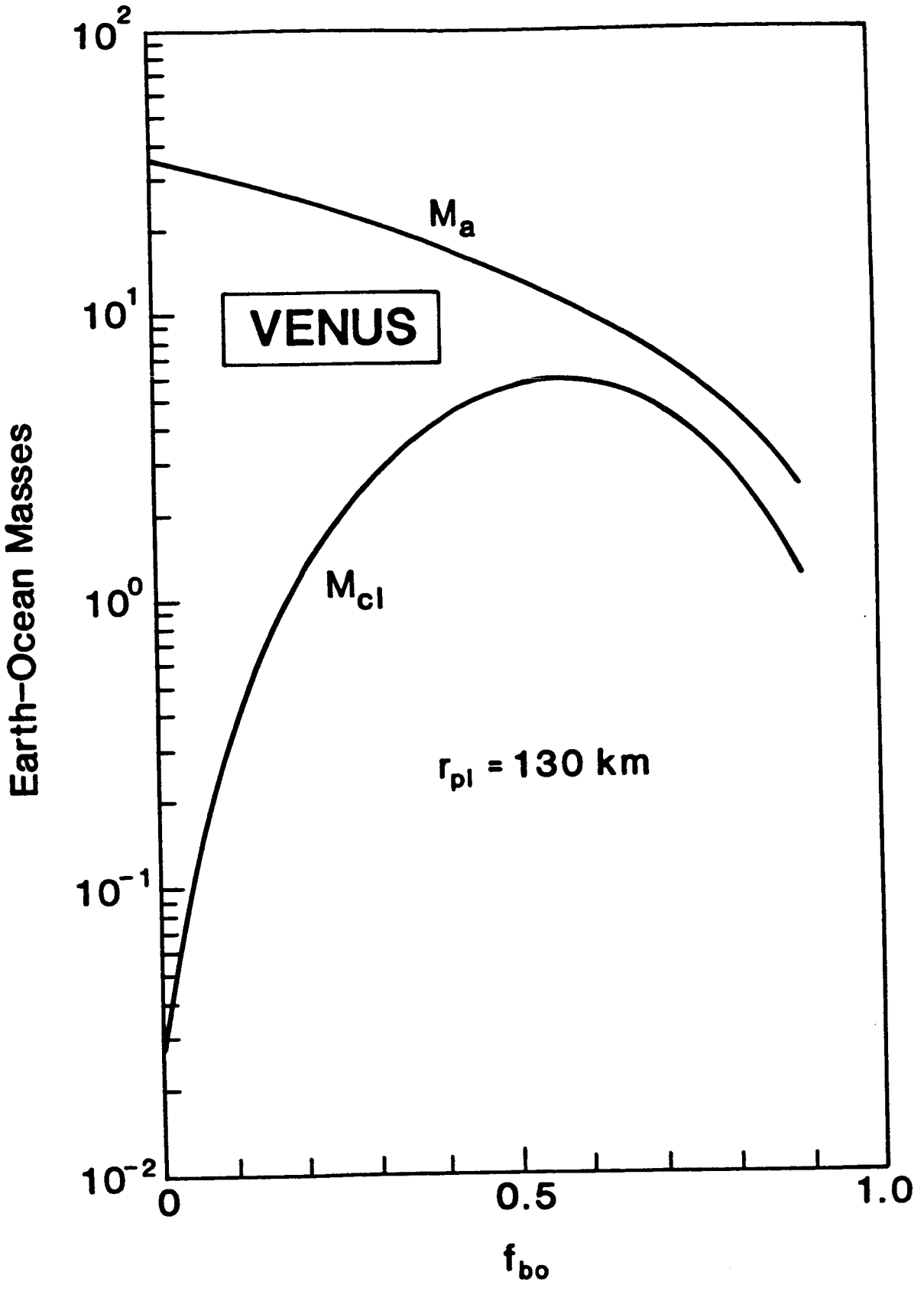

TJA88004SFD

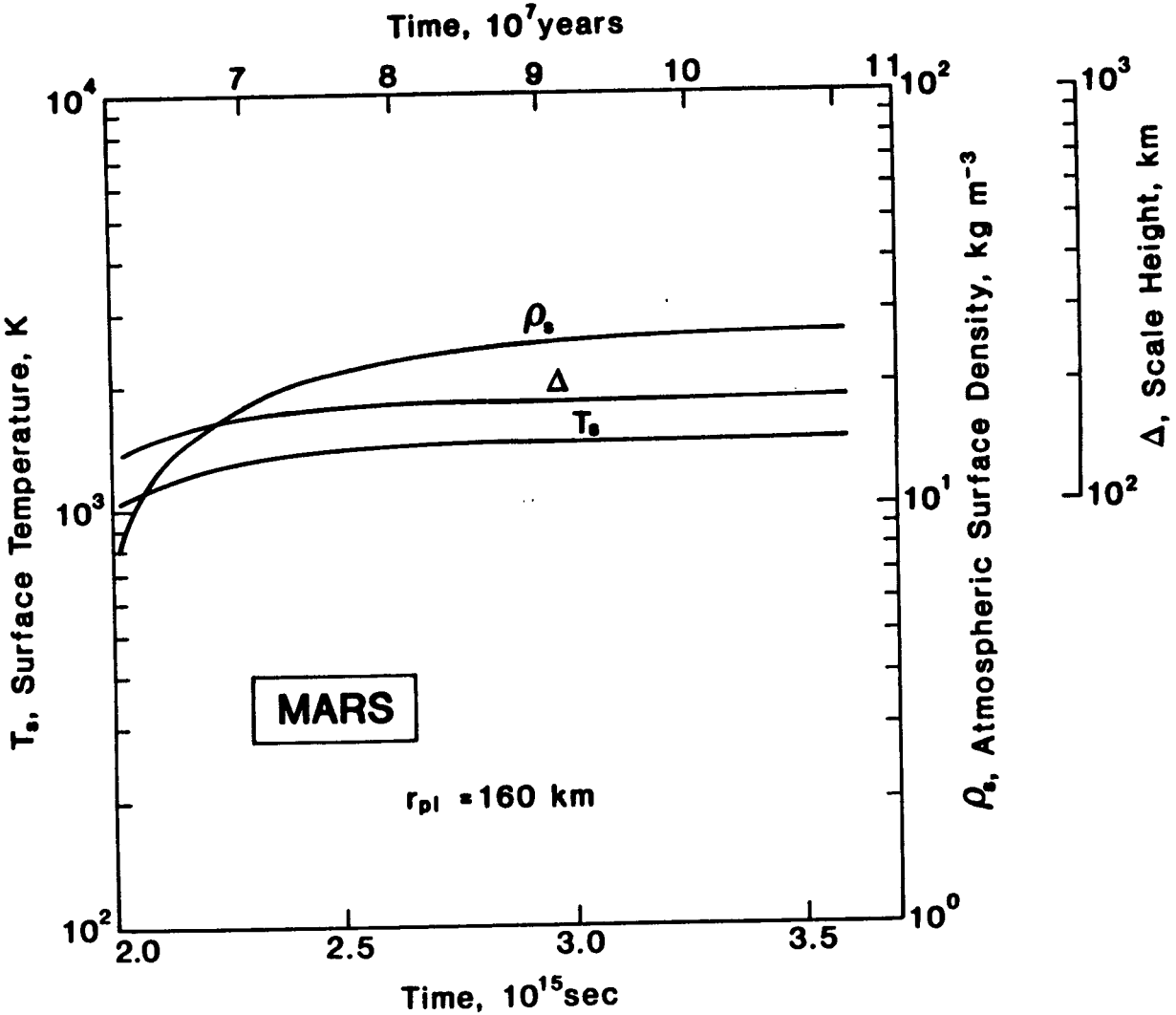
Time, 10^7 years
7
8
9
10
11
10^4
10^3
10^2
10^2
10^1
10^0
10^3
10^2
ρ_s
Δ
T_s
MARS
r_{pl} = 160 km
2.0
2.5
3.0
3.5
Time, 10^{15} sec
T_s, Surface Temperature, K
ρ_s, Atmospheric Surface Density, kg m^{-3}
Δ, Scale Height, km

TJA87172SC

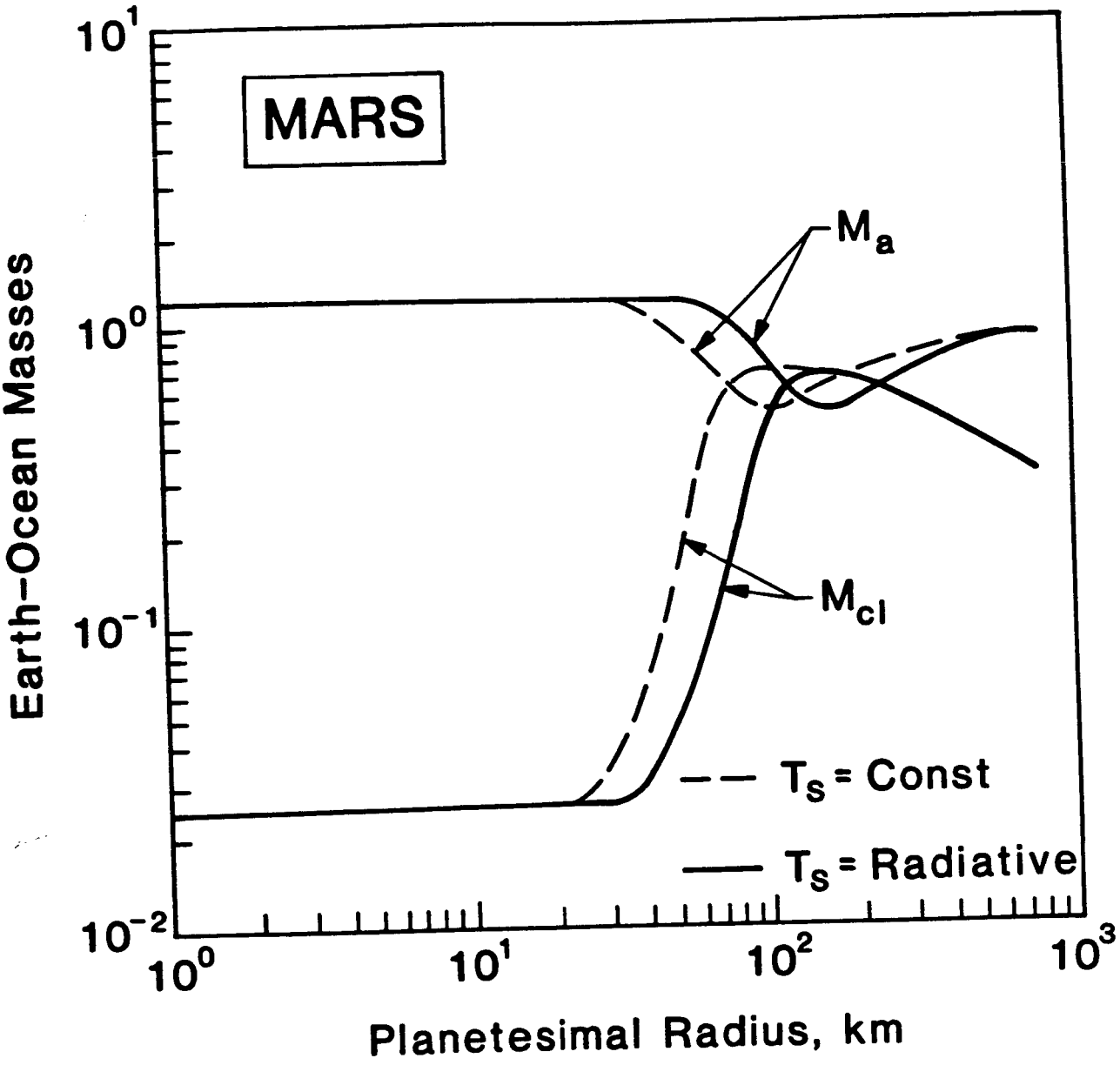

TJA87173SFD

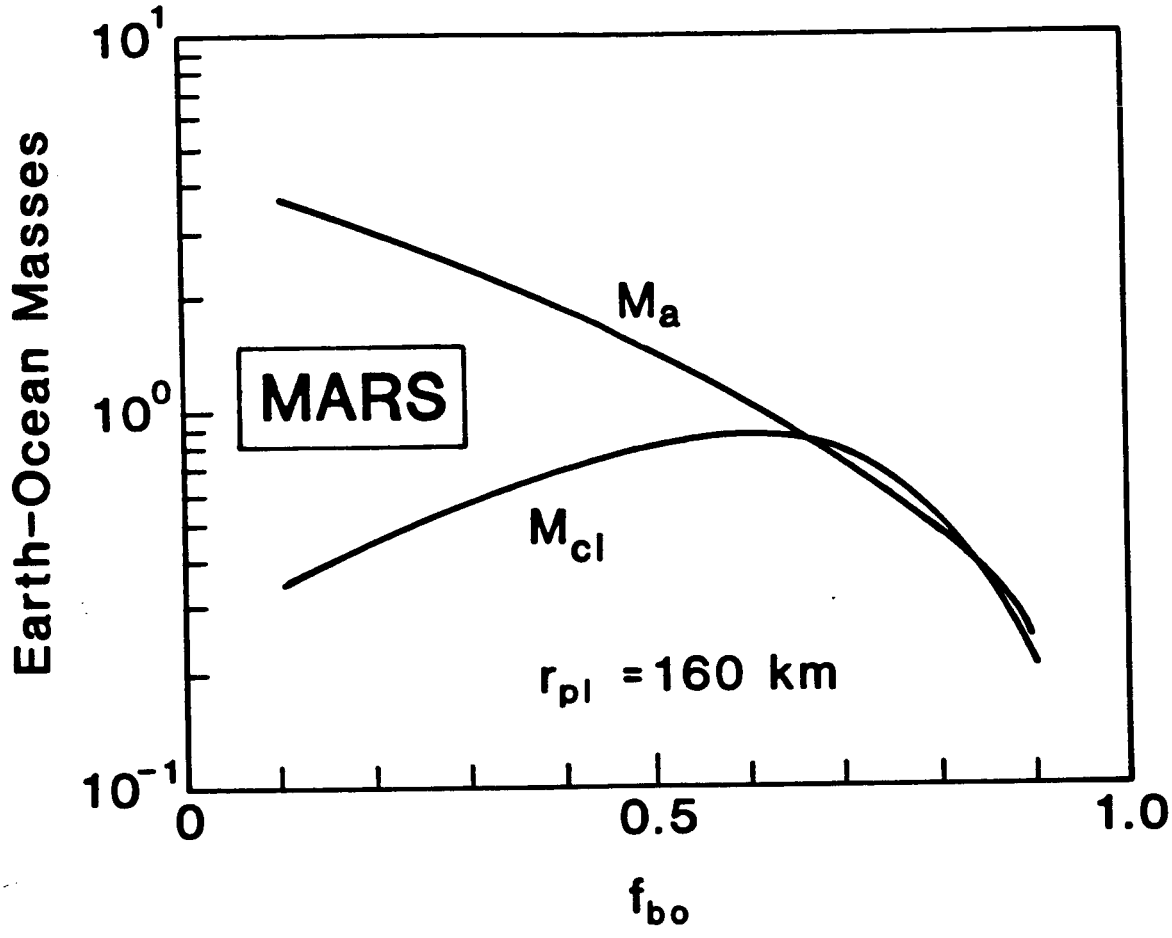

TJA87174SFD

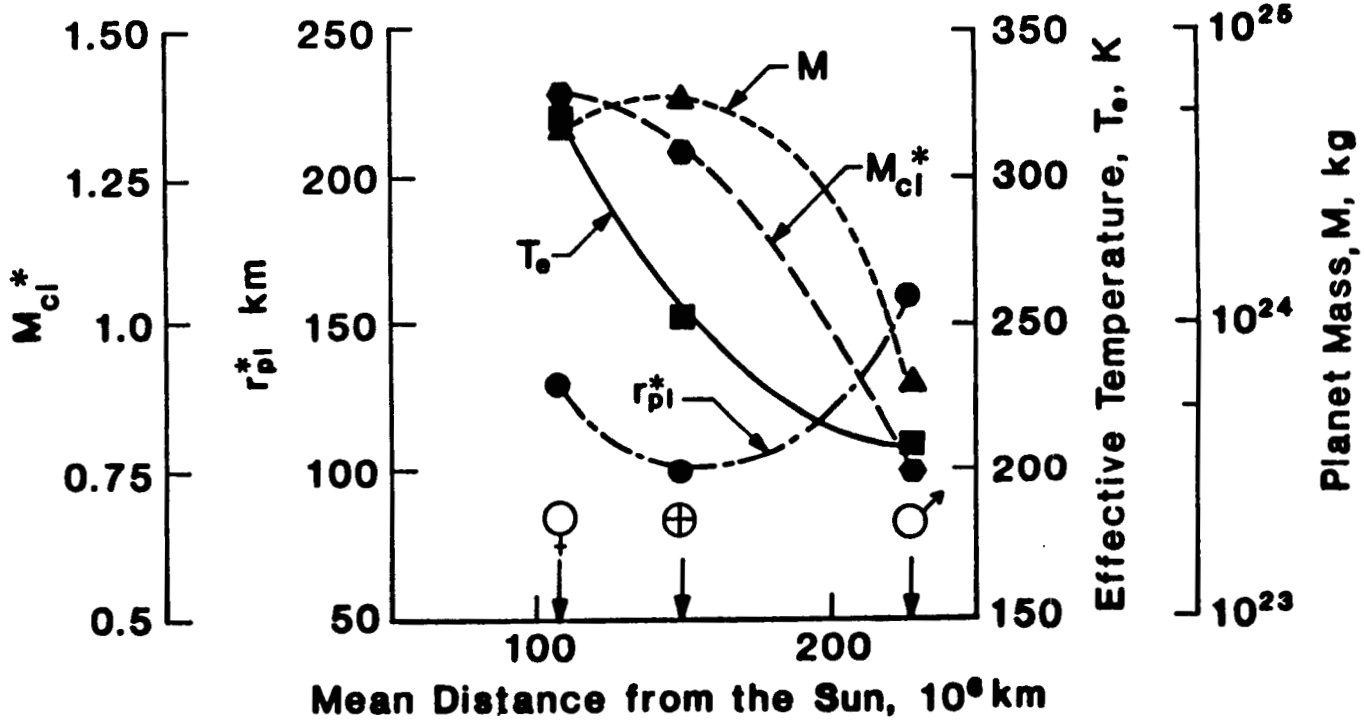
1.50
1.25
1.0
0.75
0.5
M_{cl}^*
250
200
150
100
50
r_{pl}^* km
M
M_{cl}^*
T_e
r_{pl}^*
350
300
250
200
150
Effective Temperature, T_e, K
10^{25}
10^{24}
10^{23}
Planet Mass, M, kg
100
200
Mean Distance from the Sun, 10^6 km

TJA8800SED